Mehran University Research Journal of Engineering and Technology

https://doi.org/10.22581/muet1982.3174

2025, 44(1) 82-93

Investigating the performance parameters of solar cell for efficiency enhancement

Muhammad Muneeb Khan [a, b, *], Sadiq Ahmad [b], Jahangeer Faiz [a], Rubab Nazeer [c], Muhammad Amir Shafi [d], Ahmad Bin Ishtiaq [a]

[a] *Department of Electrical Engineering and Technology, Institute of Southern Punjab Multan, 6000, Multan, Pakistan*

[b] *Department of Electrical and Computer Engineering, COMSATS University Islamabad, Wah Campus, 47040, Wahcant, Pakistan*

[c] *Department of Electrical Engineering, NFC Institute of Engineering and Technology Multan, Pakistan*

[d] *Department of Electrical and Computer Engineering, COMSATS University Islamabad, 45550, Islamabad, Pakistan*

[*] Corresponding author: Muhammad Muneeb Khan, Email: muneebkhan196@yahoo.com

Received: 10 February 2024, Accepted: 26 December 2024, Published: 01 January 2025

KEYWORDS

Thin Film Solar Cell (TFSC)

CuZnTSe thin hetero-structure

Numerical simulation

Performance Parameters

Solar cell Design

Optimized Solar Cell

ABSTRACT

Copper Zinc Tin Selenide (CuZnTSe) cells have unique physical characteristics that make them incredibly well-suited to serve as a solar material for power absorption in contemporary optimized Thin Film Solar cells (TFSC). The goal of the proposed study is to model novel hetero-structures for CuZnTSe solar cells with and without a NiO hole transport layer (HTL), namely AlZno2/Cds/CuZnTSe/Mb and Al-Zno2/Cds/CuZnTSe/Nio2/Mb. To develop and simulate the properties of the CuZnTSe cell and its possible applications in photovoltaic solar cells, simulation software SCAPS-1D is utilized. In addition to nickel oxide (NiO) serving as the electron-blocking HTL, transparent conductor oxide films such as aluminum zinc oxide (AlZnO) and cadmium sulfide (Cds) were added as electron transport layers. The incorporation of a NiO hole transport layer, carrier concentration, layer thickness, defect density, and other parameters impacting cell efficiency were all examined in this work. For the configurations under analysis, the maximum power efficiencies were 23.09% and 39.54%, respectively, with top fill-factors exceeding 79.47% and 87.21%.

1. Introduction

Escalating need for the modern and advanced renewable and limitless source of non-conventional energy sources has driven a surge of interest for increasing the efficiency of modern Thin Film Solar Cell (TFSC) within the research community [1,2]. In light of the increasing utilization and costly nature of materials like Copper Indium Gallium Sulfide (CIGS), various substitute materials with better performances have been explored [3,4]. The alteration in energy conversion effectiveness is attributed to a substantial band-offset among the interfaces of the absorber and buffer layers, denoted as offset of conduction and valence band, determinable [5]. This study focuses on analyzing a substitute material represented by the A_2BCX_4 tetra-compounds, particularly the $Cu_2ZnSnSe_4$ (CuZnTSe) Kesterite-type compounds, which exhibit an arrangement similar to Copper Indium Gallium Sulfide, Selenide cells [6]. CuZnTSe boasts the optical-gap approximately 1 electron Volt (eV), a strong capability of absorption ranging from 10^4 to 10^5 cm^{-1}, and a charge carrier density within the range of 10^{17} to 10^{20} cm^{-3} [7]. Its crystal structure closely resembles that of CIGS, that makes it very useful material for PV uses. Given its appealing characteristics and attributes, CuZnTSe emerges as a

compelling candidate for solar applications. Recognized for its availability and non-toxicity, CuZnTSe has garnered attention as a potential light-absorbing material in the development of environmentally friendly solar cells. The substance has undergone thorough examination for its utilization in thin-film solar cells [8].

Photovoltaic solar cells that are non-toxic and naturally abundant, particularly those based on CuZnTSe, have achieved noteworthy results, boasting record conversion efficiencies exceeding 11.6% [9], 13.16% [10], 14.97%, and 19.59% [24]. These findings underscore the importance of optimizing the architecture of CuZnTSe layers to achieve higher yields. Numerous research groups have employed various deposition methods for Utilizing thin layers of CuZnTSe to lower expenses and boost the power conversion efficiency of solar cells [25].

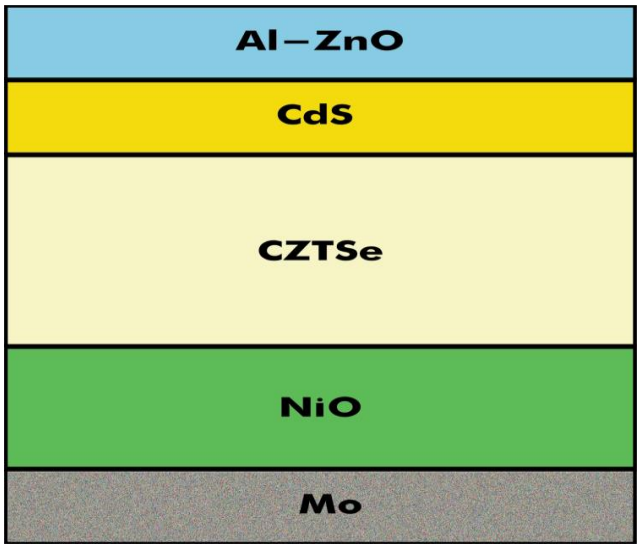

Fig. 1. Proposed Solar Cell Structure With Different Layers

Our primary tool is the Capacitance Simulator of solar cell, designed by National Instruments with Lab Windows/CVI [11-14]. Overall SCAPS-1D is a window-oriented program designed for one-dimensional solar cell structures [15,16]. It aids in the analysis and comprehension of solar cell performance. A thorough study of all films in the solar cell has been conducted by using the SCAPS-1D to simplify and improve comprehension regarding the CuZnTSe performance in solar cells and produce cells with optimal performance [17,18]. The cell thickness has been modified to attain the maximum achievable efficiency. Ensuring uniformity is maintained, the thickness of Cds buffer sheets is maintained at approximately 50 nm [15], Molybdenum functions as back contact layer (BCL). Research objective is to achieve improved performance of CuZnTSe PV cell by integrating the back contact (BC) surface layer the NiO [19-21]. It is investigated suitable BC field films and BC metals for CuZnTSe, emphasizing the film's function in restricting minority charge carriers which are participating for affective collection in p-n junction, all while avoiding an increase in the device's R_s. Confinement of photons, a crucial characteristic for an effective BC surface field layer [22,23]. Current research shows that comparing the features of two separate solar cell devices, performance parameters evaluated values such as the power conversion efficiency, fill factor, short circuit current density and open circuit voltage [26,27]. Proposed photovoltaic cell underwent adjustments by modifying the cell layer thickness, the concentration of doping, absorber layer defect density, and the integration point of Cds buffer film and CuZnTSe as an absorber film for solar cell efficiency enhancement.

2. Parameters For Material And Device Structure

The commonly employed simulation tool for investigating solar cells with max configuration is the SCAPS-1D model. It facilitates the exploration and analysis of distinctive attributes such as efficiency, fill factor, voltage and current, dependent on the inherent characteristics of CuZnTSe and NiO hole transport layer.

Table 1

Design parameters for left and right layers

Parameter	BC	FC
φ(eV)	0.5×10-1	0.04×102
Se (cm/Sec)	0.1×108	0.1×108
Sh (cm/Sec)	0.1×108	0.1×108
Rf	8.1×10-1	5×10-2

Table 2

Material proprieties for simulation design

Parameter	Ni-O	CuZnTSe	Cds	Al-ZnO
Thickness(nm)	0.4×102	1500	100	50
Eg (eV)	0.3×101	0.95	2.42	3.33
χ (eV)	0.14×101	4.6	4.4	4.55
Er	0.1×102	8.12	10	8.12
NC (1/cm3)	2.8×1019	7.9×1017	1.2×1018	4.1×1018
NV (1/cm3)	1×1019	4.5×1018	1.8×1019	8.2×1018
μn (cm2 /vs)	0.12×102	0.41×102	1×102	1×102

μp (cm2 /vs)	0.02×102	0.1×102	0.5×102	20
ND (1/cm3)	0	0	1×1019	1×1021
NA (1/cm3)	1×1021	1×1020	0	0
coefficient (cm3/s)	0.23×10-8	.23×10-14	0.23×10-8	0

Table 3

Material proprieties for solar cell design

Defects Properties	Al-ZnO	Cds	CuZnTSe [23]	NiO [26]
Defects density Nt (cm−3)	A:1017	A:1017	D:1014	D:1014
Σn (cm2)	10-12	A:10-17	A:10-15	A:10-15
Σp (cm2)	10-15	10-13	10-15	10-15
Defect type	Acceptor	Single Acceptor	Single Donor	Single Donor
Defect energy level Et	Above eV	Above eV	Above eV	Above eV
Energy level wrt refer BV	0.6	0.1	0.1	0.61

It is advisable to utilize the visual interface of SCAPS when introducing a solar cell, enabling the input of all controlled settings.

Tables 1-4 given above summarize all parameters of material employed in the simulation. Sulfide/Aluminum structure, consisting of the following layers, Fig. 1 depicts the Molybdenum/Nickel Oxide/Copper Zinc Tin Selenide/Cadmium. Tables 4 and 5 in this investigation present the Parameters at the interface and traditional defects associated with the semi-conductors used. These defects are categorized as either donor, acceptor, or neutral defects, providing valuable insights into the semiconductor material characteristics.

Table 4

Parameters used for defect density

Parameters	Cds/CuZnTSe	CuZnTSe/NiO
Defect Type	Neutral	Neutral
Capture cross sectional electrons	1×10^{-19}	1×10^{-19}
Capture cross-sectional holes	1×10^{-19}	1×10^{-19}
Defect energy level Et	high Ev	Ev
Energy with respect to Reference (eV)	6×10^{-2}	1×10^{-19}
Total density	1×10^{10}	1×10^{10}

This substance holds promise as a Hole Transport Layer for CuZnTSe solar cells owing to its significant band arrangement compatibility with the CuZnTSe cell. Within this simulation, a thorough examination was conducted on the interfaces between various layers, specifically focusing on interfaces like absorber/buffer and buffer/window.

3. Validation of Parameters through Experimental Comparison

Prior to delving into the analysis of the proposed structure, an examination of various parameters from existing literature is conducted using the simulator. Taskeen find a η of 11.4% with a Voc of 0.4 V, a Jsc of 38.1 mA/cm², and FF of 68%, notably, as compared to theoretical it presented lower efficiency from other works [15]. To understand the reasons behind the suboptimal CuZnTSe cell efficiency, we employed SCAPS-1D to match the empirical current voltage (JV) curve of CuZnTSe, which was enhanced by Taskesen. This involved considering Different experimental parameters obtained by Taskesen, including series resistance, shunt resistance, CuZnTSe carrier concentration, thickness and energy gap. Through this analysis, we obtained a PCE of 11.410%, Voc of 0.440 Voltage, Jsc of 41.620 mA/cm2, and FF of 61.170%. A noteworthy finding was a high density of CuZnTSe defects, Nt = 9×1015 cm−3, which emerged as a crucial parameter affecting efficiency. Comparing the the achieved J-V curve obtained for Molybdenum/Copper Zinc Tin Selenide/Cadmium Sulfide/Aluminum-Zinc Oxide using SCAPS-1D aligns with the experimental results, the small difference observed can be attributed to meticulous control over thickness of CuZnTSe, material defects of Eg, size of grain, and interface's defect. These factors collectively play a pivotal role in achieving closer alignment between theoretical predictions and experimental outcomes.

Table 5

Parameters of solar PV cell

Structure	Voc V	Jsc mA/cm2	FF %	η %
Cds/CuZnTSe/Mo	0.65	44.33	79.4	23.09
Cds/CuZnTSe/NiO/Mo	0.91	49.60	87.2	39.54

4. Discussion and Results

4.1 Energy Band

To optimize the CuZnTSe cell and CuZnTSe with NiO devices for maximum efficiency, the SCAPS1D program was employed. Adjustments were made to establishing the The uniformization of semiconductor film thickness is implemented to attain peak efficiency in both CuZnTSe cells and incorporating NiO layers. The proper arrangement of the energy band diagram emerges as a crucial factor affecting the movement of Photogenerated charge carriers and the whole functioning of the photovoltaic cell. The conduction band offset and valence band offset play pivotal roles in understanding the electron and hole dynamics at interfaces. In our simulations, conduction band offset between CuZnTSe and Cds was found to be 0.2 electron volt (< 0.4 eV), and VBO between CuZnTSe and Cds was calculated as -1.22 eV (< 0 eV). These values signify favorable conditions for efficient charge transfer across the interfaces.

The wider WB on the CuZnTSe side and the narrower CB contribute to the localization of holes and electrons when a junction is settled between the two materials. Notably, the substantial valence band offset between the absorber layer and buffer layers facilitates the transfer of electrons from absorber layer to buffer layer and from buffer layer to Al doped Zinc Oxide, where the collection occurs, restraining the movement of holes. However, it's crucial to acknowledge that the valence band of NiO hole transport layer is higher than optimal values, affecting the Fermi level and diminishing the open-circuit voltage VOC. While elevated CBO values greater than 0.4 eV widen the barrier preventing electron transport to the conduction band of the buffer layer, achieving a balance in these parameters is essential for optimal solar cell performance.

4.2 Current-Voltage Characteristics of CuZnTSe Thin-Layer Photovoltaic Solar Cells

Various chemical and physical techniques were employed in the fabrication of CuZnTSe solar cells, including pulse laser deposition and sputtering stacked metal precursor selenization. Previous studies show a notable cell efficiency of approximately 13.6% in the Zno / Cds /CZTS structure. To fabricate solar cells with high efficiencies and gain a deeper understanding of their performance, a numerical analysis was conducted by systematically reducing the buffer and absorber layer thickness.

The study centered on the traditional ultra-thin CuZnTSe configuration featuring a Cds buffer film, investigating both Copper Zinc Tin Selenide (CuZnTSe) and Copper Zinc Tin Selenide with Nickel Oxide (CuZnTSe/NiO) absorber layers. The SCAPS-1D was employed for simulating the property of investigating Cu2ZnSnSe4 as a tetra-component semiconductor within the Cu2 systems, this study involves the analysis of J-V curves in a thin-layer solar cell structure comprising AL-ZnO/Cds/CZTS/Mb. The solar cell's performance under diverse conditions is elucidated using the equation.

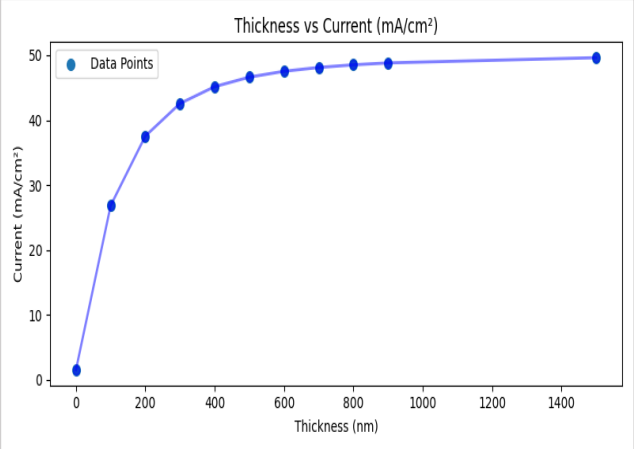

Fig. 2. Effect Of Thickness And Current For The TFSC

In this context, the idealist factor "n" corresponds to J_n, which denotes the Charge carrier density, while J_p denotes the positive charge carrier current density. Additionally, J_s represents the saturated current density, and J_w represents the current density within the depletion region. The solar cell, when in the absence of light, behaves akin to a broad, planar diode, producing the characteristics that are exponentially curved of a diode. In PN junction the p represents positive electrode region, and the n represents negative electrode region. In the darkness, it obtains very small current from minority carriers. Producing charge carriers via the absorption of incoming photons, leading to a sustained photocurrent. The JV curve will be shifted by value which is equal to I_{ph}.

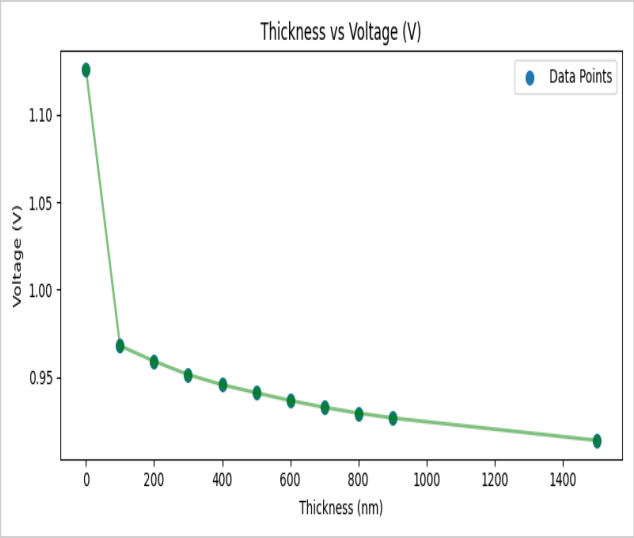

Fig. 3. Effect Of Thickness And Voltage For The TFSC

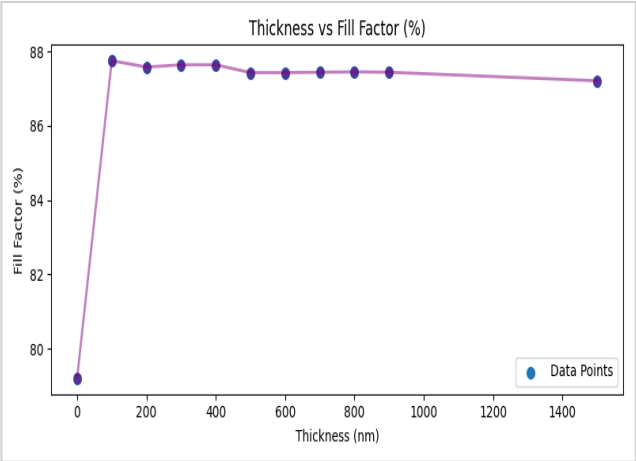

Fig. 4. Effect Of Thickness And FF For The TFSC

4.3 Absorber Film CuZnTSe Impact

Figs. 2-4 depicts the thickness parameter effect on the CuZnTSe layer. Thickness values of absorber layer is changed from 0.1 µm to 10 µm. By increasing thickness of absorber layer CuZnTSe, longer wavelengths of light are accumulated. This augmentation contributes by increasing Voc and Jsc values, primarily by the increased absorbed photons, leading to enhanced electron-hole pair generation, thereby boosting efficiency and overall device output. In In a cell featuring a slender absorber layer, the back contact is positioned near the depletion region, resulting in increased back contact recombination.

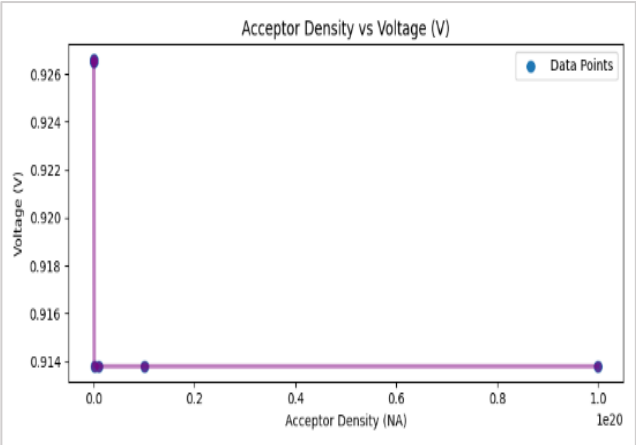

Fig. 5. Effect Of Acceptor Density NA On Voltage

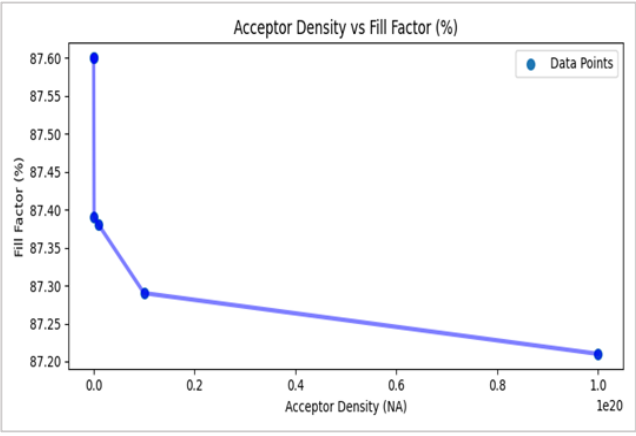

Fig. 6. Effect Of NA And Fill Factor For The TFSC

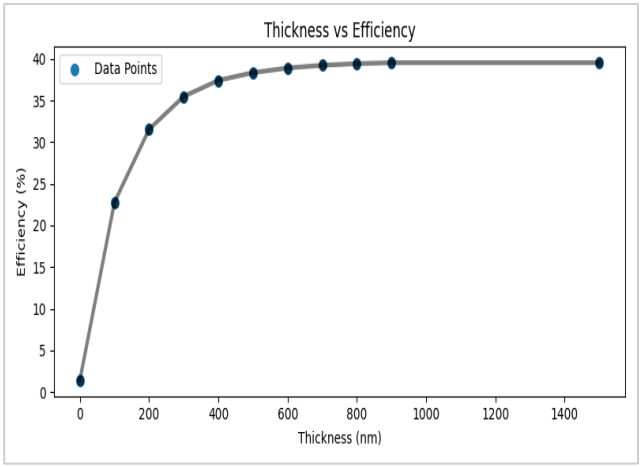

Fig. 7. Effect Of Thickness On TFSC Efficiency

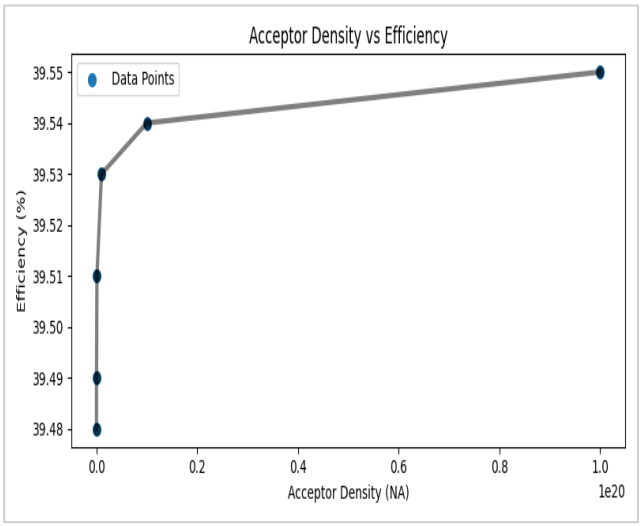

Fig. 8. NA Impact On Photo Voltaic Properties

The back-contact current decreases when the thickness of absorber layer increases, resulting in an improvement in the cell's performance. However, for thicknesses beyond 4 µm, the efficiency experiences only a modest rise and maintains relative stability. This plateau is attributed to the absorption of Photons with longer wavelengths penetrate deep into the thin absorption layer, outside the depleting area. The Quantum Efficiency (QE) spectra also exhibit a slight increase with thickness increase from 1200 nanometer (nm) of the Copper Zinc Tin Selenide (CuZnTSe) layer, this implies that only photons possessing specific energy levels exceeding the gap energy of CuZnTSe are considered for absorption, leading to the generation of electron-hole pair. The optimization of CuZnTSe thickness, it was adjusted to 0.9µm for 0.655 open circuit Voltage, and 44.33 mA/cm2 is short circuit current density, 79.47% is Fill Factor, 23.09% efficiency recorded, and NiO hole transport layer was introduced to enhance the performance. However, the inherent presence of Copper-Zinc anti-sites and copper gaps makes CuZnTSe a p-type material. As obtaining an n-type doping material is unfeasible, the charge carrier concentration was varied in the range of 2.21×1017 cm−3 to 2.21×1018 cm−3. Figs. 5-8

illustrates that at 2×1018 cm−3, both PCE and FF are maximized. The impact of thickness was simulated using the SCAPS-1D software , concentrations of charge carriers, and the density of defects impact the performance of CuZnTSe solar cells.

Beyond 5 µm thickness, the CuZnTSe characteristics stabilize. With increasing carrier concentration, the JSC decreases due to increased recombination among numerous carriers across the entire cell. An increase in doping leads to a rise in current, possibly elevating the built-in power and, consequently, the open circuit voltage. Moreover, the reduction in series resistance as carrier charge concentration increases contributes to the improvement in FF.

4.4 Impact of the Cadmium Sulphide (Cds) Thickness

In this section of our study, by analyzing how vary thickness of Cds buffer layer overall affects the performance of solar cells based on Copper Zinc Tin Selenide (CuZnTSe) within structure, by changing the thickness from 10nm to 100nm. The three crucial factors determining solar cell efficiency Voc, Jsc, and FF are under scrutiny.

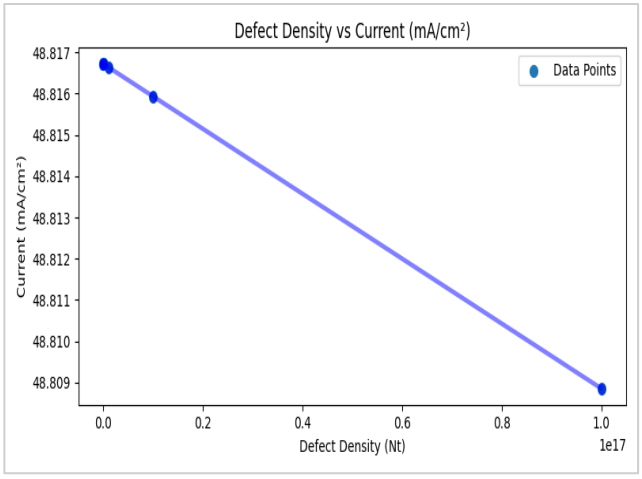

Fig. 9. Effect Of Nt On Current

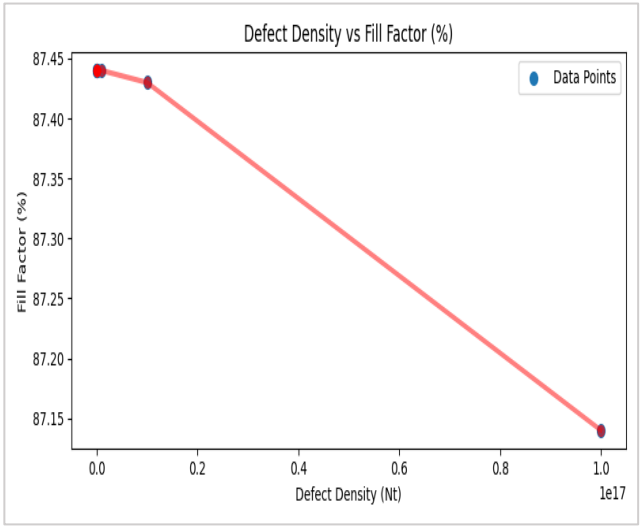

Fig. 10. Effect of Nt on FF for TFSC

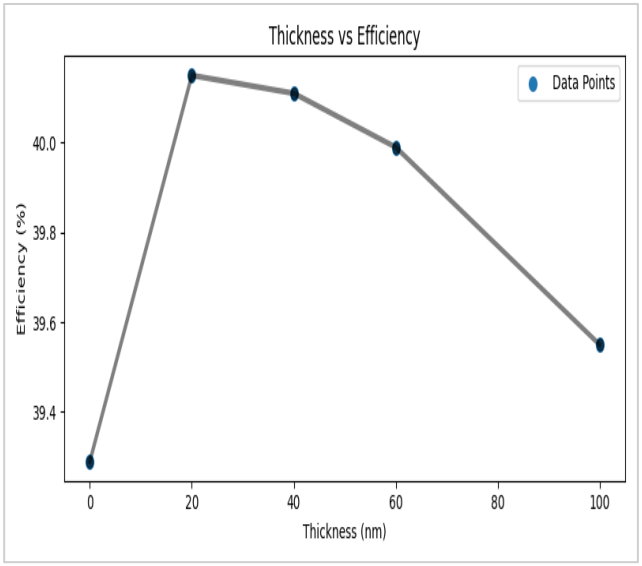

Fig. 11. Thickness vs PCE of Proposed Cell

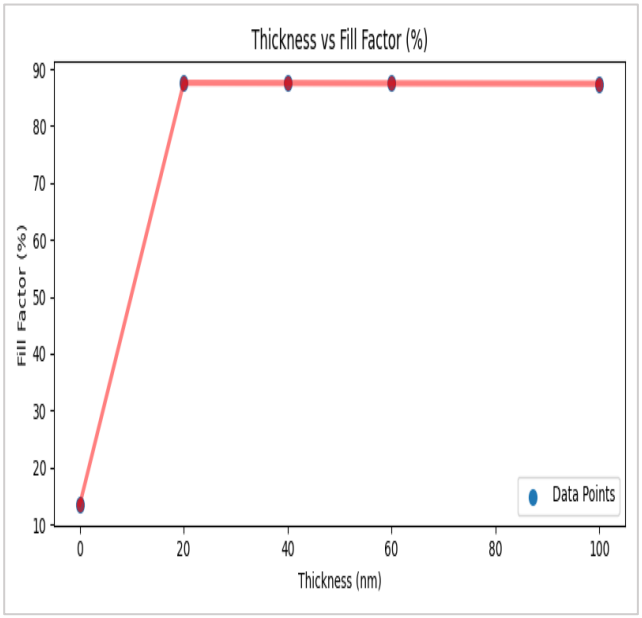

Fig. 12. Thickness vs FF of Proposed Cell

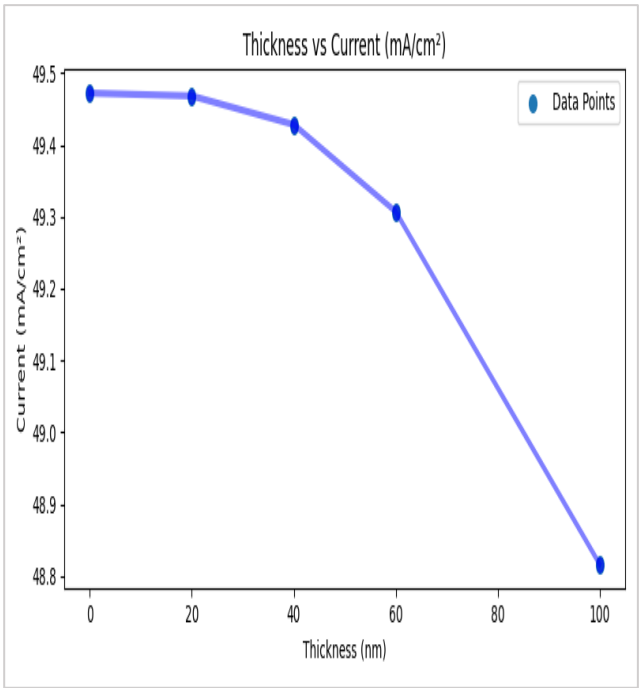

Fig. 13. Thickness vs Jsc of Proposed Cell

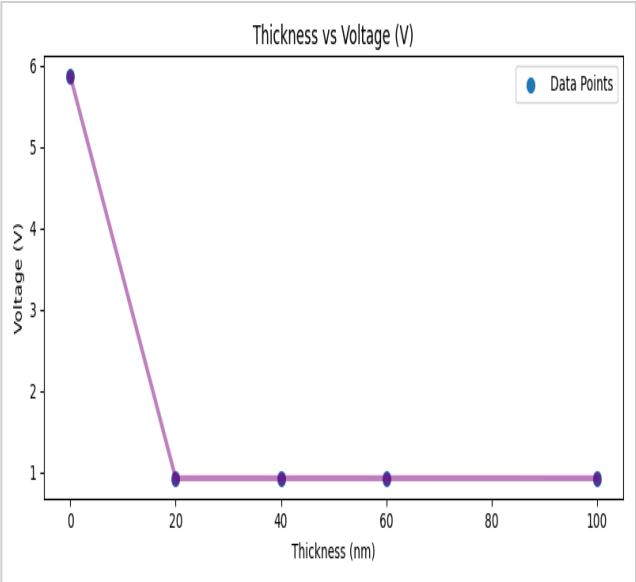

Fig. 14. Thickness vs V_{oc} of Proposed Cell

The outcomes, illustrated in Figs. 11-14, unravel the nuanced relationship between these parameters and varying Cds thicknesses. Figs. 11-14. depicts a comprehensive analysis of how altering Cds thickness affects the performance of CuZnTSe photo voltaic cells. Intriguingly, the efficiency decreases as the buffer film thickness increases up to 50 nm. However, beyond this point, the yield of the solar cells stabilizes for thickness values exceeding 50 nm. The observed efficiency decline beyond 50 nm is primarily attributed to a reduction in fill factor (FF). When buffer layer thickens increase, Photons are absorbed beyond the range of hole dispersal span. This will increase in the density of minority charge carriers, fostering higher recombination rates and, consequently, a decrease in power conversion efficiency (PCE). The reduction in PCE is further clarified by the interlayer scattering phenomena taking place among buffer as well as an absorber layers, aligning with prior findings in the literature. Examining the practical obstacles involved in manufacturing a higher quality Cds layer that is 40 nm thick and recognizing negative impact of thick buffer layers on solar cell efficiency, it becomes imperative to limit the Cds thickness to values below 100 nm.

Despite these considerations, the efficiency of the examined CuZnTSe solar cell is depicted in Figs. 11–14. Fig. 11 illustrates the relationship between thickness and PCE of the proposed solar cell, showing that with a thickness of 20 nm, the efficiency exceeds 40%. In Fig. 12, it is evident that the fill factor surpasses 85% when the thickness is greater than 20 nm. Fig. 13 demonstrates that a thickness below 20 nm results in a maximum current density of over 48%. Finally, Fig. 14 shows that the open-circuit voltage (Voc) reaches its maximum when the thickness of the proposed solar cell is kept below 20 nm.

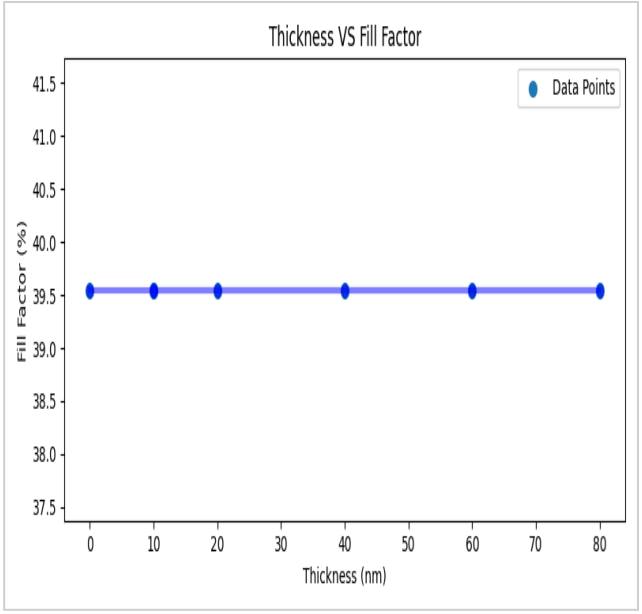

Fig. 15. Variation of Thickness on FF for NiO layer

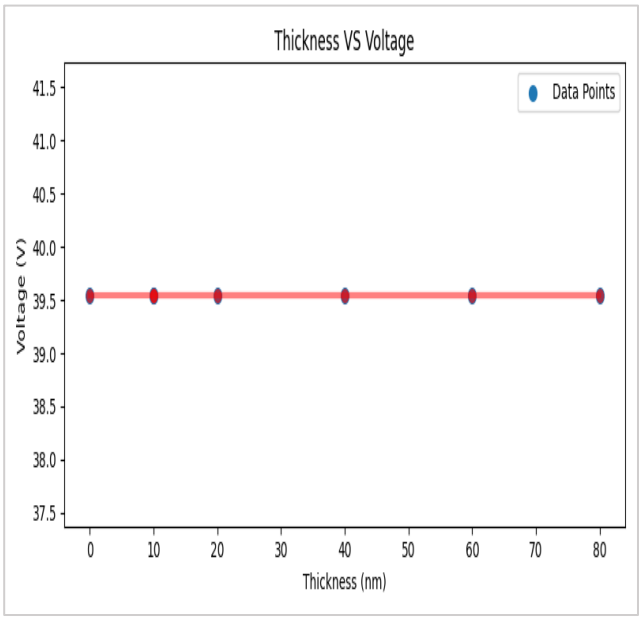

Fig. 16. Variation Of Thickness On Voc For NiO Layer

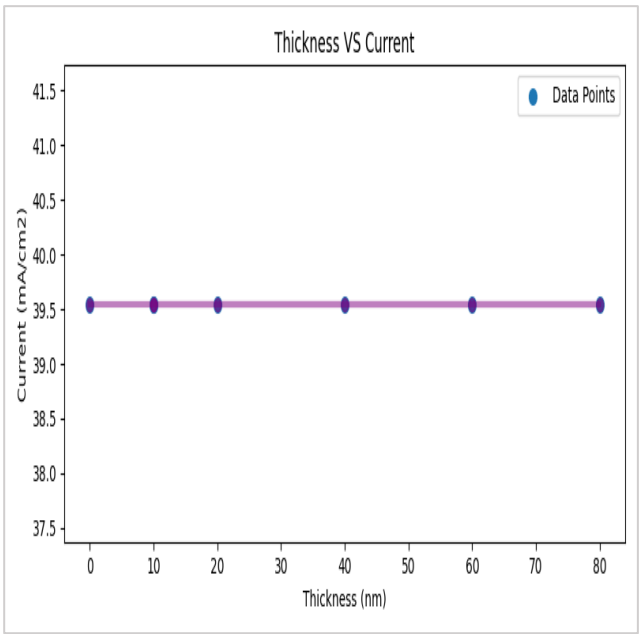

Fig. 17. Variation Of Thickness On Jsc For Nio Layer

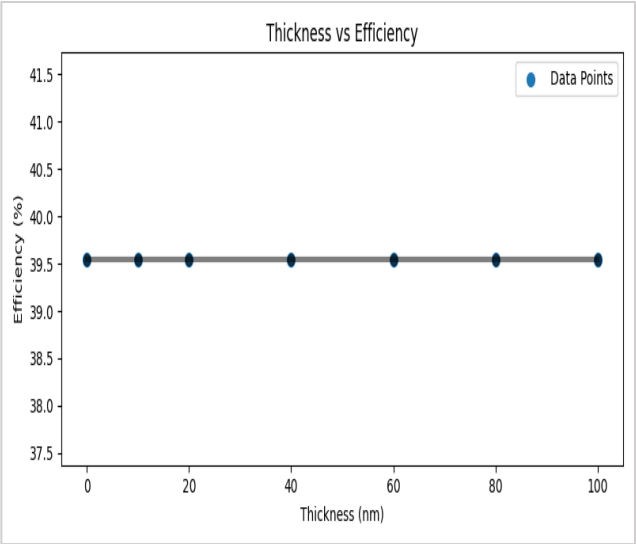

Fig. 18. Variation In Solar Cell Parameters And Comparison Of Nio B.S.F.

Layer thickness for proposed investigation is selected 80nm Cadmium Sulphide (Cds) layer thickness that have improved the efficiency of proposed SC.

4.5 Influence of the NiO HTL

The integration of a BSF into photovoltaic is crucial for creating a rear potential barrier for electrons and ensuring Ohmic response with positive charge carriers. This minimizes the likelihood of Recombination at the back contact, ultimately enhancing performance. Current research shows that by adding P-type dopping into HTL interface of CuZnTSe/Mo. By utilizing the SCAPS-1D software, we explored the influence of introducing NiO HTL as a BSF on the optimized heterostructure of CuZnTSe solar cells, we employed AlZnO/Cds/CuZnTSe/Nickel Oxide Hole Transport Layer/Molybdenum.

Figs. 15-18 illustrates novel Photovoltaic PV cell attributes of NiO HTL layer thickness. The incorporation of NiO HTL led to a significant improvement in cell performance, attributed to the beneficial alignment of the Nickel Oxide Hole Transport Layers band within Copper Zinc Tin Selenide absorbing layers. Upon incorporating NiO HTL with a 40 nm thickness of as a Back-Surface Field (BSF), the outcomes demonstrated a notable 0.9 open circuit voltage, 49.6 mA/cm2 short circuit current density, 87.21% of FF, and 39.54% of efficiency. We investigated and compared the current-voltage behavior along with the Quantum Efficiency curve of solar cells founded on Cds/CuZnTSe. The comparison involved cells with and without the integration of NiO as a HTL. NiO-HTL as a BSF resulted in an increase in QE, indicating decreased carrier reunion at the exterior of CuZnTSe and an enhancement in PCE. The summarized findings in the Table 5 showcase a significant improvement in Voc and overall PV cells performance after the integration of In solar cells based on Cds/CuZnTSe with NiO used as a HTL. Rise in Voc is credited to the suitable band alignment of the Nickel Oxide Hole Transport Layer (NiO HTL) in the envisioned heterostructure, leading to an increased band offset and, consequently, an elevated open-circuit voltage.

It is observed that the distribution profile of the electric field, when comparing configurations along with BSF layer and without BSF layer. This area serves as an obstacle for minority carriers while promoting the transport of majority carriers. The incorporation of the Back-Surface Field (BSF) layer significantly influences the Electric Field distribution near the back interface. This enhancement plays a crucial role in increasing the built-in field within the bulk of the absorber.

4.6 Effects of Parasitic Resistance

Utilizing the SCAPS-1D simulation program, we can investigate how Series Resistance Rs and Shunt Resistance Rsh influence the photovoltaic properties of the Aluminum-Zinc Oxide/Cadmium Sulfide/Copper Zinc Tin Selenide/Nickel Oxide/Molybdenum solar cell. Rs and Rsh play a crucial role in determining cell performance, affecting the shape and slope characteristics of the J-V curve. Resistance at the contacts between the layers of the solar cell, both at the front Contact FC and backside metal contacts, is ascribed to Rs, It's crucial to emphasize that Rs is correlated with the electrical resistance at the interconnections among distinct layers of the solar cell, encompassing both the FC and BC metal. Additionally, Rs contributes to electrical dissipation within the active layer and the hole transport film. Understanding these factors is crucial for optimizing the performance of the solar cell. it's important to highlight that Rsh experiences significant impact from the architectural aspects of the solar cell. This influence is derived from various charge reunion procedures, incorporating the electrical current leakage occurring along the edges of cells. A lower shunt resistance, while potentially advantageous, introduces the risk of photovoltaic leakage, potentially affecting the collected photocurrent. Understanding these dynamics is crucial for optimizing the performance of solar cells. Meanwhile, Rs primarily affects Jsc and FF values, and achieving high SC efficiency requires a low Rs and a relatively high Rsh.

In examining the impact on the solar cell's performance within the AlZnO/ Cds/CuZnTSe/NiO/Mb structure, by varying Rs from

0 to 34 Ωcm2 and Rsh from 100 to 1500 Ωcm. The evolution of key photovoltaic parameters for the studied solar cell was examined. An increase in Rs values led to a reduction in all PV parameters, except for VOC, which exhibited independent behavior to Rs. Conversely, PCE and FF increased with rising Rsh, stabilizing for higher values. VOC showed a slight effect from Rsh, and JSC demonstrated an independent behavior. The influence of Rs is linked to the resistance within the material's bulk and the impedance characteristics of electrodes and other materials. It's crucial to emphasize that the solar cell functions primarily as a voltage source, and the series resistance R_s has no impact on the open-circuit voltage V_{OC}. A significant increase in the V_{oc} correlates with a decrease in the magnitude of the J_{SC}. The PCE as well as FF of investigated solar cell fluctuate with its Shunt Resistance, where a higher R_{sh} leads to an increased power output. Therefore, to enhance the performance of photovoltaic cells and reduce losses, it is crucial to decrease R_s and elevate R_{sh}.

Table 6 Benchmarking against previous studies

PV Structure	Study	PV Parameters				References
		Jsc	V	FF	η	
CuZnTSe/Cds	Simulation	44.3	0.65	79.4	23.09	Proposed Work
CuZnTSe/Cds	Simulation	44.8	0.55	52.1	13.16	[23]
CuZnTSe/Cds	Simulation	39.9	0.66	75.3	19.59	[24]

4.7 Impact of Operating Temperature on Solar Cell Performance

Throughout the simulation analyses conducted, we adhered to an ambient temperature of 300 K, which is the conventional temperature for solar cell testing in manufacturing practices.

Table 7

Benchmarking against previous studies

PV Structure	Study Type	PV Parameters Jsc (mA/cm2)	Voc (V)	FF (%)	H (%)	References
CuZnTSe /NiO	Simulation	45.42	0.835	86.48	39.54	This Work
CuZnTSe /NiO	Simulation	28.3	1.211	83.81	25.31	[26]

To gain deeper insights into the temperature's influence on our cells' performance, given the frequent outdoor installation of solar panels, we investigated how the operating temperature affects the performance of the CuZnTSe device. By maintaining the constancy, of all optimized parameters, introducing variability only in the operational temperature. This variation ranged from 250 K to 400 K while ensuring a consistent illumination level of 1000 W/m2. Observations indicate that the open-circuit voltage (V_{OC}) decreases with an increase in working temperature, showcasing a rate of change dependent on temperature. As the temperature rises, cells characteristics decrease, except for the J_{SC}, which exhibits an increase. The heightened temperature provides additional energy to electrons in the device, leading to an increased generation of electron-hole pairs and consequently boosting J_{SC}. Material characteristics, including band gap, carrier charge concentration, and the mobility of holes and electrons, undergo changes that lead to a reduced conversion efficiency of the solar cell. it's crucial to acknowledge that the heightened operating temperature plays a significant role in altering material conductivity. This alteration is attributed to the increased diffusion of charge carriers facilitated by phonons thermal activation, resulting in a decline in the PV cell's efficiency. Understanding these temperature-induced effects is pivotal for optimizing the efficiency of our solar cell configurations. Therefore, an elevated working temperature tends to decrease the overall efficiency of the solar cell. Conversely, at lower operating temperatures, the device demonstrates superior performance.

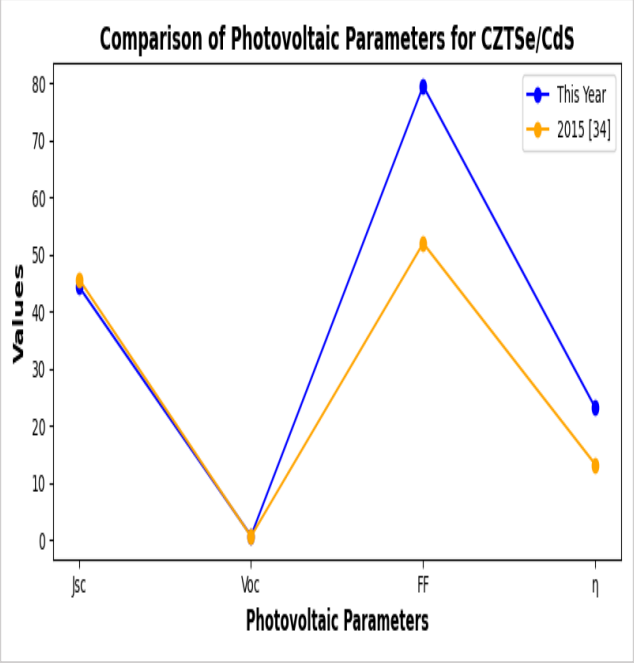

Fig. 19. Comparison With Previous Work

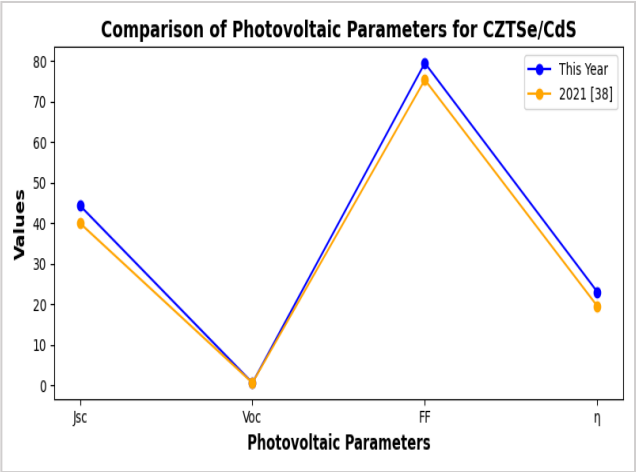

Fig. 20. Comparison With Previous Work CuZnTSe/Cds

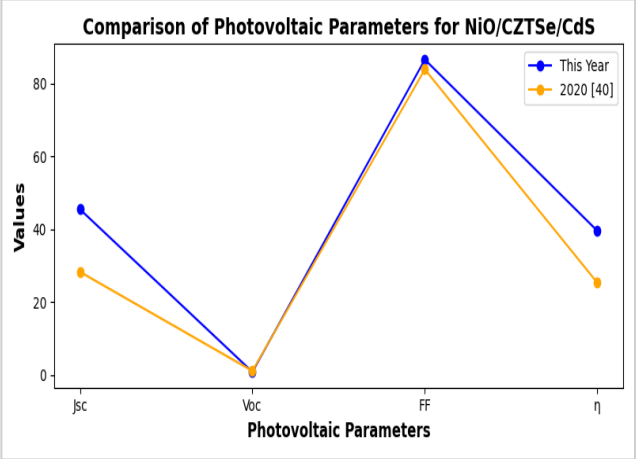

Fig. 21. Comparison With Previous Work NiO/CuZnTSe/Cd

5. Comparative Analysis

In this segment, we carried out a comparative investigation, benchmarking the higher efficiency value achieved in our study against values explained in the existing literature. As delineated in Table 6, the solar cell with the CuZnTSe/Cds (η = 23.09%) Outperforming comparable setups, our optimized parameters demonstrate superior performance, including CuZnTSe/ZnSe and CuZnTSe/Cds heterostructures depicted in Figs. 19-21. Defects and impurities within CuZnTSe layers may impose limitations on the theoretical PCE of CuZnTSe, factors meticulously considered in our simulation. it's essential to highlight the critical role of both the buffer layer type (Cds, ZnSe) and the thickness of CuZnTSe. These factors are pivotal for enhancing the production of electrons and holes, influencing the overall performance of the solar cell.

Moreover, Table 7 illustrates the impact of interlayers on the characteristics of the CuZnTSe absorbent layer. Introducing NiO in the form of a hole transport layer between Mo and CuZnTSe demonstrated its efficacy as an interlayer, leading to improvements in the characteristics of absorber film.

6. Conclusion

This work provides a comprehensive numerical analysis using the SCAPS-1D software simulation, focusing on a solar cell constructed using the combination Cu2ZnSnSe4 (CuZnTSe). The natural availability and affordability of CuZnTSe make it a promising material for solar applications. In order to gain a thorough grasp of how thickness variation and acceptor copper zinc tin selenium density affect our solar cell designs, the inquiry started with an analysis of the suggested cell AlZnO/Cds/CuZnTSe/Mb. The structure AlZincOxide/Cadmium Sulfide/Copper Zinc Tin Selenide/Nickel Oxide/Molybdenum was then created by integrating NiO HTL in the form of BSF after an analysis was done to determine the impact of the thickness of the Cds buffer film. The addition of the Nickel Oxide Hole Transport Layer significantly increased the efficiency of the cells, as demonstrated by the Copper Zinc Tin Selenide solar cell's outstanding 23.09% efficiency jump. Without the Nickel Oxide Hole Transport Layer, characteristics including resistances Rs and Rsh and a Jsc of 49.60 mA/cm2 were analyzed. High solar cell yield has been shown to be influenced by low series resistance and high shunt resistance. The study also looked at how operating temperature impacts PV cell efficiency. It found that higher temperatures reduced device efficiency, highlighting the need of lower operating temperatures for best results. Our technique was proven to be accurate and reliable when our simulations were compared to the literature already in existence. This paper shows several important junction topologies and offers useful insights for experimental experiments using hetero-Copper Zinc Tin Selenide and Nickel Oxide Hole Transport Layers.

7. References

[1] H. Arbouz, A. Aissat, J. P. Vilcot, "Simulation and optimization of Cds-n/ Cu2ZnSnS4 structure for solar cell applications", Int. J. Hydrogen Energy 42 (13), 8827–8832. 2017.

[2] M. M. Khan, S. Ahmad, H. Sikandar, B. Akram, M. Hussain, “Simulation Design of a Photovoltaic based reliable Street Lighting System using PVSyst Software” IEEE-International Conference on Emerging Trends in Smart Technologies (ICETST), 2024. DOI: 10.1109/ICETST62952.2024.10737942

[3] G. A. Casas, M. Á. Cappelletti, A. P. Cedola, B. M. Soucase, EL. P. Y. Blancá, " Analysis of the power conversion efficiency of perovskite solar cells with different materials as Hole-Transport Layer by numerical simulations", Superlattices

and Microstructures, Vol. 107, pp. 136-143, 2017.

[4] M. M. M. Khan “Enhancing Distributed Generation in Remote Areas of Sindh and Balochistan through Optimized Sizing of Grid Connected Photovoltaic Systems” IEEE International Conference on Emerging Trends in Smart Technologies (ICETST), 2024. DOI: 10.1109/ICETST62952.2024.10737943

[5] M. M. Khan, M. A. Shafi, N. Khan, "Development of prototype of grid tie inverter (grid synchronization and load sharing)", International Journal of Engineering and Advanced Technology (IJEAT), Volume 05, Issue 05, 2016.

[6] S. Ahmmed, A. Aktar, M. F. Rahman, J. Hossain, A. B. M. Ismail, "A numerical simulation of high efficiency Cds/CdTe based solar cell using NiO HTL and ZnO TCO", Optik 223, 165625. 2020.

[7] S. Ahmmed, A. Aktar, M. F. Rahman, J. Hossain, A. B. M. Ismail, "Enhancing the open circuit voltage of the SnS based heterojunction solar cell using NiO HTL", Solar Energy 207, 693–702. 2020.

[8] H. Arbouz, A. Aissat, J. P. Vilcot, "Simulation and optimization of cds-n/ cu2znsns4 structure for solar cell applications", Int. J. Hydrogen Energy 42 (13), 8827–8832. 2017.

[9] M. M. Khan, S. Ahmad, R. G. Hassan, M. A. Shafi, B. M. Soucase, "Ideal tilt angle of a photovoltaic system to enhance sustainability of the educational buildings", Southern Journal of Engineering & Technology, Special Issue, Vol. 01, Issue 01, 2024.

[10] L. Et-taya, T. Ouslimane, A. Benami, "Numerical analysis of earth-abundant cu2znsn (sxse1-x) 4 solar cells based on spectroscopic ellipsometry results by using SCAPS-1D", Sol. Energy 201, 827–835, 2020.

[11] S. Mohammad nejad, Z. M. Bahnamiri, S. E. Maklavani, "Enhancement of the performance of kesterite thin-film solar cells using dual absorber and ZnMgO buffer layers", Superlattices Microstruct. 144, 106587. 2020.

[12] K. Mukhopadhyay, P. Fermi Hilbert Inbaraj, J. Joseph Prince, "Thickness optimization of cds/zno hybrid buffer layer in CuZnTSe thin film solar cells using SCAPS simulation program", Mater. Res. Innovations 23 (6), 319–329. 2019.

[13] T. Taskesen, J. Neerken, J. Schoneberg, D. Pareek, V. Steininger, J. Parisi, L. Gütay, "Device characteristics of an 11.4% CuZnTSe solar cell fabricated from sputtered precursors", Adv. Energy Mater. 8 (16), 1703295. 2018.

[14] S. Mohammad nejad, Z. M. Bahnamiri, S. E. Maklavani, "Enhancement of the performance of kesterite thin-film solar cells using dual absorber and ZnMgO buffer layers", Superlattices Micro struct. 144, 106587. 2020.

[15] M. A. Shafi, S. Bibi, M. M. Khan, H. Sikandar, F. Javed, H. Ullah, L. Khan, B. M. Soucase, "A numerical simulation for efficiency enhancement of CZTS based thin film solar cell using SCAPS-1D", East European Journal of Physics, 2022.

[16] M. A. Shafi, M. M. Khan, S. Bibi, M. Y. Shafi, N. Rabbani, H. Ullah, L. Khan, B. M. Soucase, "Effect of parasitic parameters and environmental conditions on IV and PV characteristics of 1D5P model solar pv cell using LTSPICE-IV", East European Journal of Physics, 2022.

[17] M. M. Khan, S. Ahmad, S. Jabbar, S. Baloch, M. A. Shafi, R. Nazeer, J. Faiz, "Simulation design of grid tied photovoltaic (PV) system of a 1.05 kWp DC for a geographical location of Tandojam, Sindh", 1st International Conference on Women Development WD-EST’23, October, 2023.

[18] M. M. Khan, S. Ahmad, M. U. Tariq, Z. H. Anjum, M. A. Shafi, "Simulation design of 542kWp DC/480kWp AC solar photovoltaic system at Institute of Southern Punjab", Sir Syed University Research Journal of Engineering & Technology, Vol. 14, No.1, 2024.

[19] M. M. Khan, A. Rasheed, M. A. Shafi, “Array Tilt Angles to Maximize Solar Power Generation Efficiency” IEEE International Conference on Emerging Trends in Smart Technologies (ICETST), 2024. DOI: 10.1109/ICETST62952.2024.10737963

[20] W. Wang, M. T. Winkler, O. Gunawan, T. Gokmen, T. K. Todorov, Y. U. Zhu, D. B. Mitzi, "Device characteristics of CZTSSe thin-film solar cells with 12.6% efficiency", Adv. Energy Mater. 4 (7), 1301465. 2014.

[21] M. M. Khan, B. Akram, M. A. Shafi, S. Jabbar, J. Faiz, and R. Nazeer, "Design and simulation of photovoltaic power park for evacuating Sindh

solar potential using HVDC transmission system", 13th Int. Mech Eng Conference, NED UET Karachi, pp. 1-6, 6-8 March 2024.

[22] M. M. Khan, S. Ahmad, H. Sikandar, M. Hussain, B. Akram, A. Raza, "Design and assessment of photovoltaic power generation potential in Pakistan's South Punjab", 2nd International Multidisciplinary Conference on Emerging Trends in Engineering Technology (2nd IMCEET), BBUSTSD, March, 2024.

[23] M. M. Khan, S. Ahmad, A. Raza, R. G. Hassan, U. Tariq, H. Sikandar, M. A. Shafi, "Optimized photovoltaic system using PV syst software for residential building energy in Multan", Southern Journal of Engineering & Technology, 2(1), 63-73, 2024.

[24] A. Srivastava, P. Dua, T. R. Lenka, S. K. Tripathy, "Numerical simulations on CZTS/CuZnTSe based solar cell with ZnSe as an alternative buffer layer using SCAPS1D", Mater. Today. Proc. 43, 3735–3739, 2021.

[25] K. J. Yang, D. H. Son, S. J. Sung, J. H. Sim, Y. Kim, S. N. Park, "A band-gap-graded CZTSSe solar cell with 12.3% efficiency", Journal of Material Chemistry. A. 4 (2016) 10151–10158.

[26] S. Ahmmed, A. Aktar, M. F. Rahman, J. Hossain, A. B. M. Ismail, "A numerical simulation of high efficiency cds/cdte based solar cell using NiO HTL and ZnO TCO", Optik 223, 165625. 2020.

[27] M. M. Khan, S. Ahmad, M. S. Iqbal, H. Sikandar, R. G. Hassan, M. A. Shafi, "Performance analysis of PVSyst based grid connected photovoltaic systems in Pakistan compared to SAARC countries", Mehran University Research Journal of Engineering and Technology (MURJET), Vol. 43(2), 2024.

